ELSEVIER

Nuclear Physics B 563 (1999) 97–106

NUCLEAR PHYSICS B

www.elsevier.nl/locate/npe

New limits on spin-dependent coupled WIMPs and on 2β processes in ^{40}Ca and ^{46}Ca by using low radioactive CaF_2(Eu) crystal scintillators

P. Belli [a], R. Bernabei [a], C.J. Dai [b], F. Grianti [c], H.L. He [b], G. Ignesti [d], A. Incicchitti [d], H.H. Kuang [b], J.M. Ma [b], F. Montecchia [a], O.A. Ponkratenko [e], D. Prosperi [d], V.I. Tretyak [e], Yu.G. Zdesenko [e]

[a] *Dip. di Fisica, Universita' di Roma ''Tor Vergata'' and INFN, sez. Roma2, I-00133 Rome, Italy*
[b] *IHEP, Chinese Academy, P.O. Box 918/3, Beijing 100039, China*
[c] *Istituto di Fisica, Universitá di Urbino and INFN, sez. Bologna, Italy*
[d] *Dip. di Fisica, Universita' di Roma ''La Sapienza'' and INFN, sez. Roma, I-00185 Rome, Italy*
[e] *Institute for Nuclear Research, 252680 Kiev, Ukraine*

Received 2 June 1999; received in revised form 16 September 1999; accepted 20 September 1999

Abstract

The development of highly radio pure CaF_2(Eu) crystal scintillators has been performed aiming at a substantial sensitivity enhancement of the 2β decay investigation and of the search for dark matter particles with spin-dependent (SD) interaction. The results of CaF_2(Eu) background measurements and simulation are presented. New and highly improved $T_{1/2}$ limits on the 2β decay of ^{46}Ca and the double electron capture of ^{40}Ca are obtained as well as further results on SD coupled WIMPs.

PACS: 23.40.-s; 95.35.+d; 29.40.Mc
Keywords: Double beta decay; Dark matter; Scintillation detectors

1. Introduction

The investigations of the neutrinoless (0ν) double β decay (which violates the lepton number conservation) is a powerful tool to search for information leading to possible new physics beyond the standard model [1–4]. Moreover, at present, the $0\nu 2\beta$ decay is also considered a powerful test for different extensions of the standard model (including several SUSY models), which could offer not only complementary but – in some cases – competitive and superior results than other running or forthcoming accelerator and non-accelerator experiments [4–6].

The most sensitive results in the search for the 2β decay have been obtained by the so-called ''active source'' technique; in this case, the detector, which contains the 2β

0550-3213/99/$ - see front matter
PII: S0550-3213(99)00618-5

decay candidate nuclei, serves itself as source [1–3]. This approach provides much higher detection efficiency and density of the candidate nuclei than the ''passive source'' technique, where a thin source is separated from the detector. For instance, we can compare the 100% efficiency quoted for Ge semiconductor detectors in Ref. [7] with the 4% efficiency of the NEMO2 tracking detector searching for the $2\nu 2\beta$ decay of ^{100}Mo [11] and of ^{116}Cd [12].

As examples of the results achieved with the ''active source'' technique, we recall the highest half-life limit $T_{1/2} > 1.1 \times 10^{25}$ y ($m_\nu < 1$ eV) established for ^{76}Ge (enriched HP Ge detectors) [7] and the $T_{1/2}$ limits in the range 3×10^{22} y–4×10^{23} y ($m_\nu < 2$–4 eV) obtained for ^{136}Xe (high pressure Xe TPC) [8], for ^{130}Te (low temperature bolometers) [9] and for ^{116}Cd (enriched $^{116}CdWO_4$ scintillators) [10].

Simple considerations can easily demonstrate that progress in the 2β decay research is directly connected with the development of ''active'' detectors.

Suitable detectors for 2β decay studies are the well known calcium fluoride scintillators [13,14]. In fact, they have a relatively large light output ($\simeq$ 60% of NaI(Tl)) and offer excellent operational characteristics (non-hygroscopicity, inertness, insolubility, good mechanical properties, etc.) when used as β particles or low energy radiation detectors [14–16]. In particular, they can be usefully utilized to search for the 2β decays of ^{46}Ca (natural abundance: $\delta = 0.004\%$; $Q_{\beta\beta} = 990.4$ keV) and of ^{48}Ca ($\delta = 0.187\%$; $Q_{\beta\beta} = 4272$ keV) besides the double electron capture of ^{40}Ca ($\delta = 96.941\%$; $Q_{2EC} = 193.8$ keV). The first experiment of this kind regarded the 2β decay of ^{48}Ca [17]; let us also mention the latest ones on the 2β decay of ^{48}Ca [18], of ^{46}Ca [19,20] and on the double electron capture of ^{40}Ca [21].

Moreover, the CaF_2(Eu) detectors have been considered as promising detectors for the direct search of Dark Matter particles with SD coupling [21,22]. In fact, the CaF_2(Eu) contains ^{19}F nuclei ($\delta = 100\%$) with non-zero spin ($J = 1/2$), for which a relatively large cross section for SD coupling has been calculated [23].

All the considerations mentioned above motivated the R&D program for the development of radio pure calcium fluoride detectors carried out by the DAMA collaboration with the Bicron company [19–21]; the aim was to enhance the sensitivity of searches for 2β decay and dark matter particles with SD interaction. We present here a new step of development performed in the framework of this R&D program and devoted mainly to the study of the CaF_2(Eu) background and to the understanding of its origins. New results on 2β decay processes and on the search for dark matter particles with SD interaction are also given.

2. Measurements

Two CaF_2(Eu) crystals grown by the Bicron company were used in the present work. Each crystal has 3″ diameter by 1″ length (370 g mass). These crystals are labelled in the following as Bicron-1 and Bicron-2.

The background measurements have been performed in the Gran Sasso underground laboratory inside the R&D DAMA set-up described in Ref. [21] for the Bicron-1 test. Here we only recall the main features of the apparatus for the measurements performed with Bicron-2. The crystal was coupled to a low background PMT EMI9265B53/FL

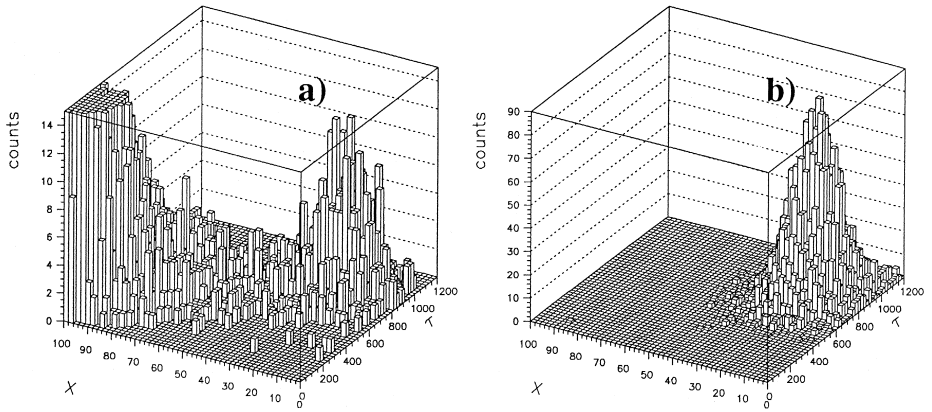

Fig. 1. Examples of bidimensional plots for residual noise rejection (see text); (a) from production data in the lowest energy region; (b) from ^{241}Am source data in the same experimental condition and energy range as the production ones.

through a 10 cm long TETRASIL-B light guide; it was wrapped by a teflon diffuser ($\simeq 100\,\mu$m thick) as also the light guide. The detector and the PMT were inside about 10 cm of low radioactive copper shaped in order to contain them tight. We note that in this measurement no NaI(Tl) anti-Compton detector was used as instead done in the Bicron-1 data taking [21]. The detector and the $\simeq 10$ cm Cu envelop were closed inside a sealed low radioactive Cu box, in one turn surrounded by a shield made of 10 cm of low radioactive copper and 15 cm of low radioactive lead followed by 1.5 mm Cd foil and about 4/10 cm of polyethylene/paraffin. To avoid any contact with environmental air (which can contain radon in trace), the Cu box was continuously flushed with high purity (HP) nitrogen gas (long stored deep underground) and maintained at about 1 mbar overpressure. Finally, the whole shield was sealed in a plexiglass box also maintained in HP nitrogen atmosphere.

The rejection of the residual noise just above the software energy threshold (4 keV here)[1] profits by the different timing structure between the noise (PMT fast signals with decay times of order of tens ns) and the CaF_2(Eu) ''scintillation'' (signals with decay times of order of 940 ns) pulses, whose shapes were recorded over 3125 ns by a Lecroy Transient digitizer. Several variables with different expected values for noise and scintillation events can be built from the recorded shapes. In particular, the comparison – for each event – between the value of the first momentum of the pulse time distribution calculated within 2500 ns (τ)[2] and the value assumed by the variable $X = 100 \cdot \frac{\text{Pulse-Area}(0-100\,\text{ns})}{\text{Pulse-Area}(0-1000\,\text{ns})}$ resulted well effective. Examples of distributions for production (a) and source (b) data in the interesting low energy region are shown in Fig. 1. The residual noise can be rejected from the production data by applying software cuts; the

[1] We recall that in any kind of experiment requiring an energy threshold at keV level, software cuts or – sometimes – hardware procedures near threshold have to be applied, although generally the corresponding procedures are not explicitly quantified by the authors.

[2] τ will be exactly the decay constant of the pulse in case of pure exponential shape, when considering an infinite averaging time.

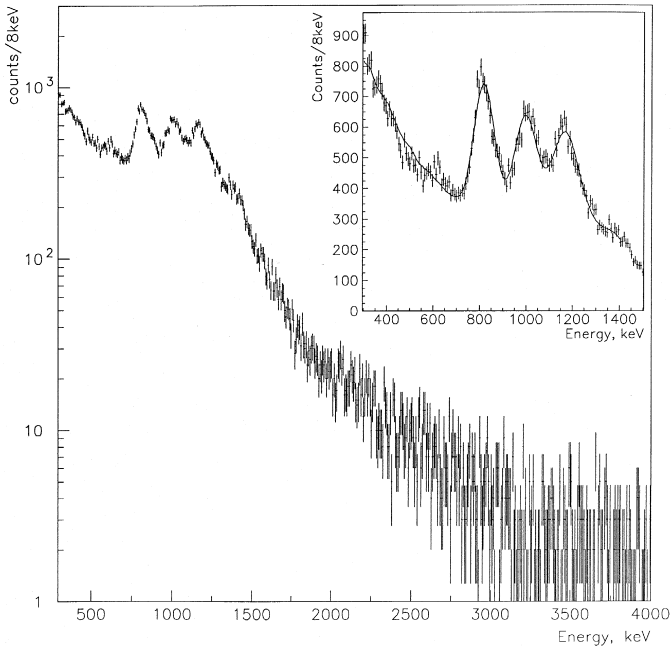

Fig. 2. Measured background spectrum of the Bicron-2 crystal for the energy region 300–4000 keV. The three peaks at about 0.81, 1.01 and 1.15 MeV can be ascribed to α-particles from ^{232}Th and ^{238}U chains internal impurities of the crystal. In the insert the fitting of the α peaks is shown.

corresponding software cut efficiency for each energy bin can be evaluated by applying the same cuts to the source data (collected in the same experimental conditions and energy range).

The background spectrum of the Bicron-2 crystal was measured in this apparatus during 1906.3 h in the three energy regions: 4–20 keV, 40–230 keV and 200–4000 keV. Data previously collected with Bicron-1 were also available for analysis; the measuring time was 631.4 h for the energy interval 4–24 keV and 260.9 h for the energy region 200–3300 keV [21].

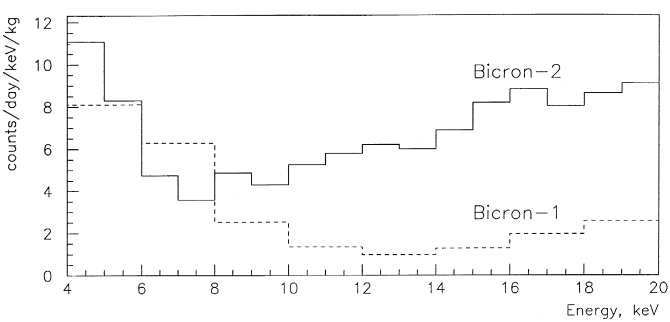

Fig. 3. Measured background spectra of the Bicron-2 and Bicron-1 crystals for the energy region 4–20 keV.

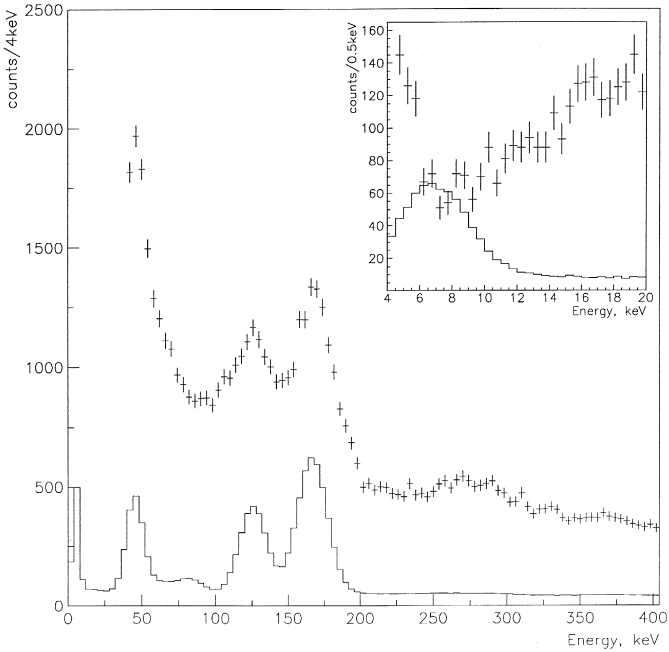

Fig. 4. Experimental spectrum of the Bicron-2 crystal up to the energy of 400 keV. The three peaks at $\simeq 47$ keV, $\simeq 129$ keV and $\simeq 169$ keV can be ascribed to ^{152}Eu ($T_{1/2} = 13$ y) activity created in the CaF_2(Eu) crystal by the neutron activation at Earth surface. The model distribution from ^{152}Eu contamination is also shown (see text for details).

During the measurement, the energy scale and resolution of the detector were calibrated periodically with different sources: ^{109}Cd ($E_\gamma = 22$ keV); ^{137}Cs ($E_\gamma = 32$; 662 keV); ^{22}Na ($E_\gamma = 511$; 1275 keV) and ^{60}Co ($E_\gamma = 1173$; 1332 keV). In addition, background peaks ($E_\gamma = 128$ and 169 keV) from ^{152}Eu contamination in the Bicron-2 crystal were used for calibration in the energy region 40–230 keV.

The measured background spectrum of Bicron-2 crystal in the energy region 300–4000 keV is shown in Fig. 2, while the low energy part (4–20 keV) and the middle energy (40–400 keV) are given in Figs. 3 and 4, respectively. Three peaks at the energies of about 0.81, 1.01 and 1.15 MeV are present; considering the typical α/β ratio for the light output of the CaF_2(Eu) crystals, these peaks can be attributed to α-particles due to ^{232}Th and ^{238}U internal impurities. Moreover, in the lower energy region, three clear peaks at energies $\simeq 47$ keV, $\simeq 129$ keV and $\simeq 169$ keV are also present. As shown by simulation (see below), such peaks could be explained by ^{152}Eu ($T_{1/2} = 13$ y) activity created in the CaF_2(Eu) crystal by the neutron activation at the Earth's surface.

3. Background simulation and estimate of the 2β decay half-life limits

The locations and amounts of the radioactive contaminations have been estimated by simulating the background spectra of the CaF_2(Eu) crystal by the GEANT3.21 package

[24] and the event generator DECAY4 [25–27], which describes the initial kinematics of the events. The considered background model includes external (from the ^{40}K, ^{232}Th and ^{238}U contaminations in the PMT) and internal (from ^{40}K, ^{152}Eu, ^{232}Th and ^{238}U intrinsic impurities in the CaF_2(Eu) crystal) contributions; it was supposed that equilibrium in U and Th chains may be broken. The fit of the experimental spectrum in the energy interval 40–2700 keV following this model gives the activities of the possible impurities in PMT and in crystal; these are shown in Table 1. As is evident, the equilibrium in U and Th chains for the CaF_2(Eu) contaminations is broken, as often in detectors.

The fit in the energy interval 300–1500 keV is shown together with the experimental data in the insert of Fig. 2, where a reasonable agreement is achieved. Also the energy dependence of the α/β ratio for the CaF_2(Eu) crystal was obtained $\alpha/\beta = 0.130 + 0.017 \cdot E_\alpha$, where E_α is the energy of the α particle in MeV.

The experimental spectrum up to the energy 400 keV is given in Fig. 4. There is also shown the model distribution from ^{152}Eu contamination, which consists of four peaks at the energies: (a) $\simeq 7$ keV (L-shell binding energy of Sm); (b) $\simeq 47$ keV (K-shell binding energy of Sm); (c) $\simeq 128.8$ keV (sum of L-shell binding energy with the most intensive $\simeq 121.8$ keV γ-ray or conversion electron from ^{152}Eu decay); (d) $\simeq 168.8$ keV (sum of K-shell binding energy with the $\simeq 121.8$ keV γ-ray). The absence in the data of the $\simeq 7$ keV peak (see also Fig. 3) could be explained by the known cross sections uncertainties ($\pm$ 10%) in the low energy region 40–120 keV, which were used for simulation. The estimated activity of the ^{152}Eu in the Bicron-2 crystal – considering the higher energy peaks – is 7.5(20) mBq/kg. Such activity could be reached after approximately five months of activation of the CaF_2(Eu) crystal (in our case the content of Eu is $\simeq 0.5\%$ [28]) at Earth surface, where the thermal neutron flux is about 5×10^{-3} neutrons/cm^2/s.

The background model described above was used to estimate half-life limits for the double EC capture of ^{40}Ca ($Q_{2EC} = 193.8$ keV) and the neutrinoless double β decay of ^{46}Ca ($Q_{\beta\beta} = 990.4$ keV). The number of candidate nuclei in each CaF_2(Eu) crystal is equal to 2.766×10^{24} and 1.141×10^{20} for ^{40}Ca and ^{46}Ca, respectively. The double EC capture of ^{40}Ca has to be followed by the emission of two X-rays with 3.2 keV energy each and it is expected that an inner bremsstrahlung photon will carry off the energy released in the neutrinoless process. Efficiencies for the different double β decay processes were calculated by using the GEANT3.21 package [24] and the event generator DECAY4 [25–27]; their values are shown in Table 2 for the given energy intervals. The measured background rates in the same energy intervals are also reported.

Table 1
Radioactive impurities of the PMT and CaF_2(Eu) crystal (mBq/kg)

Source of background	^{232}Th-chain		^{238}U-chain				^{152}Eu	^{40}K
	^{232}Th	^{228}Ra	^{238}U	^{230}Th	^{226}Ra	^{210}Pb		
PMT	<100	–	–	–	400(200)	–	–	$4(2)\times10^4$
CaF_2(Eu) Bicron-2	1.2(5)	11(5)	0.5(2)	4.5(8)	2.4(10)	0.5(2)	7.5(20)	5(2)

Table 2
Calculated efficiencies for the different double β decay processes. η_Σ is the total efficiency: $\eta_\Sigma = \eta_{\Delta E} \cdot \eta_{KK} \cdot \eta_{FA}$, where η_{KK} is the probability of double K-capture (there could be K+K; K+L and L+L emissions; because $\eta_K = 0.9$, thus $\eta_{KK} = 0.81$); η_{FA} is the probability of the full absorption peak. For instance, for $0\nu 2$EC of ^{40}Ca (6.4 keV) – it is the probability that the bremsstrahlung photon will escape the crystal and two 3.2 keV X-rays will be absorbed; in case of $0\nu 2$EC of ^{40}Ca (193.8 keV) – it is the probability that the bremsstrahlung photon and the two 3.2 keV X-rays will be fully absorbed in the crystal. $\eta_{\Delta E}$ is the efficiency of the chosen energy window. B2 and B1 are the averaged background rates in the considered energy windows given in cpd/kg/keV for the Bicron-2 and Bicron-1 crystals, respectively

2β process (Peak energy)	Energy window (keV)	FWHM (keV)	$\eta_{\Delta E}$	η_{KK}	η_{FA}	η_Σ	B2	B1
$0\nu 2$EC of ^{40}Ca (6.4 keV)	4–10	4.4	0.87	0.81	0.499	0.35	6.0	5.6
$0\nu 2$EC of ^{40}Ca (193.8 keV)	175–212	26.2	0.90	–	0.12	0.11	6.3	–
$2\nu 2$EC of ^{40}Ca (6.4 keV)	4–10	4.4	0.87	0.81	1.00	0.70	6.0	5.6
$0\nu 2\beta$ of ^{46}Ca (990 keV)	945–1036	65	0.90	–	0.95	0.86	2.4	1.3

The simulated response functions of $CaF_2(Eu)$ crystals and the calculated values of efficiencies for the different 2β decay processes were used together with the corresponding background rates, the measuring times and the numbers of ^{40}Ca and ^{46}Ca nuclei in order to estimate half-life limits for the effects under investigation. These limits are summarized in Table 3 and were obtained in two different ways. Firstly, they have been obtained by using the so-called ''one σ approach'', in which the excluded number of signal events is determined simply as the square root of the number of background counts in a given energy window ΔE. Notwithstanding its simplicity, this method gives the right scale of the experiment's sensitivity. Moreover, the $T_{1/2}$ limits were improved by using the standard procedure of the least square fit of the experimental data by the

Table 3
Half-life limits for different 2β processes of ^{40}Ca and ^{46}Ca

2β process (Peak energy)	$T_{1/2}$ limit, y (one σ approach) 68% C.L.		$T_{1/2}$ limit, y (χ^2 fit procedure) 68% (90%) C.L.		$T_{1/2}$ limit, y (χ^2 fit procedure) 68% (90%) C.L. (Combined from Bicron-1 + Bicron-2)
	Bicron-2	Bicron-1	Bicron-2	Bicron-1	
$0\nu 2$EC of ^{40}Ca (6.4 keV)	4.4×10^{21}	2.7×10^{21}	$4.1(2.5)\times10^{21}$	$2.4(1.4)\times10^{21}$	$4.9(3.0)\times10^{21}$
$0\nu 2$EC of ^{40}Ca (193.8 keV)	5.5×10^{20}	–	$3.4(1.8)\times10^{20}$	–	$3.4(1.8)\times10^{20}$
$2\nu 2$EC of ^{40}Ca (6.4 keV)	8.8×10^{21}	5.3×10^{21}	$8.2(5.0)\times10^{21}$	$4.8(2.8)\times10^{21}$	$9.8(5.9)\times10^{21}$
$0\nu 2\beta$ of ^{46}Ca (990 keV)	1.8×10^{17}	9.1×10^{16}	$1.5(0.9)\times10^{17}$	$8.3(4.9)\times10^{16}$	$1.7(1.0)\times10^{17}$

sum of the background model and of the simulated response function of the detector for the 2β decay process under investigation. From such a fit, the number of events in the expected signal peak (and the uncertainty) were determined, usually giving no statistical evidence for the effect. Then using these values, the excluded – at 68% (90%) C.L. – numbers of events for the different 2β decay processes were calculated in accordance with the Particle Data Group procedure [29].

As an example, part of the experimental spectrum of the crystal Bicron-2 in the energy interval 4–20 keV and the fitting curve are shown in Fig. 5, where the excluded – at 90% C.L. – peak from the $0\nu 2$EC decay of ^{40}Ca with half-life 2.5×10^{21} y is also shown.

In the last column of Table 3 the half-life limits obtained by combining the results for both crystals: Bicron-2 and Bicron-1 [21] are shown. In this case the procedure was as follows. The numbers of events in the expected peak – determined for each crystals by χ^2 fit as described above – were simply added: $S = S_1 + S_2$, while their error bars were added quadratically: $\sigma(S) = [\sigma^2(S_1) + \sigma^2(S_2)]^{1/2}$. The values of S and $\sigma(S)$ were used to calculate the combined excluded numbers of events for different 2β decay processes.

The $T_{1/2}$ limit obtained for $0\nu 2\beta$ decay of ^{46}Ca is higher than the best result previously available [19,20]. Restriction for the two neutrino 2EC of ^{40}Ca is also improved from value 4.6×10^{21} y [21] to $\simeq 10^{22}$ y. It should be stressed that the last one is the highest half-life limit obtained up-to-date for the $2\beta^+$ decay processes and, in

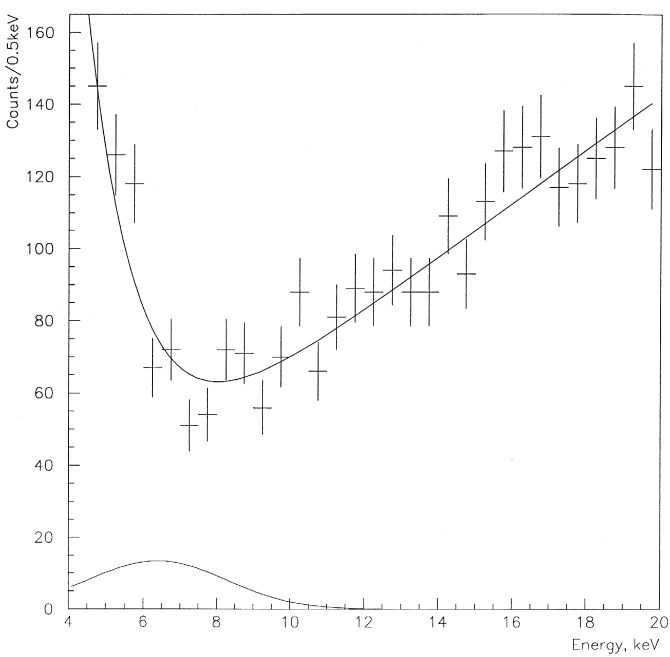

Fig. 5. The 4–20 keV experimental energy spectrum of the Bicron-2 crystal and the fitting curve, where the excluded – at 90% C.L. – peak from $0\nu 2$EC of ^{40}Ca with half-life 2.5×10^{21} y is also shown.

particular, for the double electron capture (see reviews [1–3] and Ref. [30] for comparison). The same is true for the neutrinoless 2EC of ^{40}Ca, whose $T_{1/2}$ limit is established for the first time.

4. Results on spin-dependent coupled WIMPs

In Fig. 3 the energy spectra measured by Bicron-1 and Bicron-2 in the 4–20 keV energy region are compared; the quoted rates have already been corrected for the needed efficiencies. Some slight differences are present in the two distributions and can be ascribed both to differences in the procedures for their realization and to different running conditions (see Section 2). However, the sensitivities reached in the two cases are largely similar.

Here we present the result obtained when combining the Bicron-1 and Bicron-2 data (OR-ed); the exclusion plot at 90% C.L. in the WIMP-nucleon cross section (σ_p) versus WIMP mass (M_W) has been derived for WIMP-^{19}F elastic scattering (see Fig. 6). It has been calculated according to the astrophysical and nuclear physics considerations and to the parameters' values given in Ref. [21]. For comparison the DAMA/CaF_2-1 result of Ref. [21] is also shown.

We comment here that – in spite of the favourable SD cross section for ^{19}F – further efforts on the radio purification of the CaF_2(Eu) scintillators are necessary to improve the presently best available limits for SD dark matter particles achieved with NaI(Tl) [31] and liquid Xenon scintillators [32] by employing the pulse shape discrimination of the electromagnetic background.

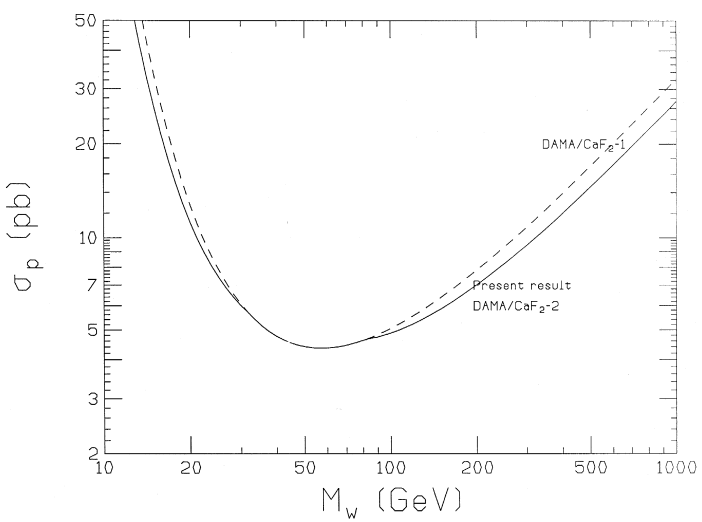

Fig. 6. The present result (OR-ed Bicron-1 and Bicron-2 data) for spin-dependent WIMP-nucleon elastic scattering; the exclusion plot is at 90% C.L. It is compared with the previous result DAMA/CaF_2-1 of Ref. [21] (see text for comment).

5. Conclusions

The new and highly improved $T_{1/2}$ limits on the 2β decay processes of ^{46}Ca and ^{40}Ca achieved here have surely demonstrated the feasibility and perspectives of developed CaF_2(Eu) scintillators for high sensitive investigations of the 2β decay. The use of these scintillators in the search for dark matter particles with SD coupling is also another interesting possibility.

Further efforts are in progress.

References

[1] M. Moe, P. Vogel, Ann. Rev. Nucl. Part. Sci. 44 (1994) 247.
[2] V.I. Tretyak, Yu.G. Zdesenko, At. Data Nucl. Data Tables 61 (1995) 43.
[3] J. Suhonen, O. Civitarese, Phys. Rep. 300 (1998) 123.
[4] H.V. Klapdor-Kleingrothaus *et al.*, J. Phys. G: Nucl. Part. Phys. 24 (1998) 483.
[5] V.A. Bednyakov *et al.*, Mod. Phys. Lett. A 12 (1997) 233.
[6] M. Hirsch, H.V. Klapdor-Kleingrothaus, Prog. Part. Nucl. Phys. 40 (1998) 323.
[7] L. Baudis *et al.*, Phys. Lett. B 407 (1997) 219.
[8] R. Luescher *et al.*, Phys. Lett. B 434 (1998) 407.
[9] A. Alessandrello *et al.*, Phys. Lett. B 433 (1998) 156.
[10] F.A. Danevich *et al.*, Nucl. Phys. B (Proc. Suppl.) 70 (1999) 246.
[11] D. Dassie *et al.*, Phys. Rev. D 51 (1995) 2090.
[12] R. Arnold *et al.*, Z. Phys. C 72 (1996) 239.
[13] G.F. Knoll, Radiation Detection and Measurement, 2nd ed. (New York, 1989).
[14] C. Colmenares *et al.*, Nucl. Instrum. Methods 114 (1974) 277.
[15] M. Campbell *et al.*, Nucl. Instrum. Methods 137 (1976) 235.
[16] J. Pouliot *et al.*, Nucl. Instrum. Methods 270 (1988) 69.
[17] E. Der Mateosian, M. Holdhaber, Phys. Rev. 146 (1966) 810.
[18] K. You *et al.*, Phys. Lett. B 265 (1991) 53.
[19] R. Bernabei *et al.*, Il Nuovo. Cim. A 111 (1998) 347.
[20] R. Bernabei et al., Il Nuovo Cim. A, Oct. 1998.
[21] R. Bernabei *et al.*, Astroparticle Phys. 7 (1997) 73.
[22] C. Bacci *et al.*, Astroparticle Phys. 2 (1994) 117.
[23] J. Ellis, R.A. Flores, Phys. Lett. B 263 (1991) 259.
[24] R. Brun et al., CERN Program Library Long Writeup W5013, CERN, 1994.
[25] Yu. G. Zdesenko et al., Preprint KINR 89-7, Kiev, 1989.
[26] V.I. Tretyak, Preprint KINR 92-8, Kiev, 1992.
[27] O.A. Ponkratenko et al., to be published.
[28] D. Krus, Bicron co., private communication.
[29] Particle Data Group: Review of Particle Physics, Phys. Rev. D 54 (1996) 1.
[30] P. Belli *et al.*, Astroparticle Phys. 10 (1999) 115.
[31] R. Bernabei *et al.*, Phys. Lett. B 389 (1996) 757.
[32] R. Bernabei *et al.*, Phys. Lett. B 436 (1998) 379.